

SELF-AFFINE FRACTALS OF FINITE TYPE

CHRISTOPH BANDT

*Institute for Mathematics, Arndt University,
17487 Greifswald, Germany
E-mail: bandt@uni-greifswald.de*

MATHIAS MESING

*Institute for Mathematics, Arndt University,
17487 Greifswald, Germany
E-mail: mesing@daad-alumni.de*

Abstract. In the class of self-affine sets on \mathbb{R}^n we study a subclass for which the geometry is rather tractable. A type is a standardized position of two intersecting pieces. For a self-affine tiling, this can be identified with an edge or vertex type. We assume that the number of types is finite. We study the topology of such fractals and their boundary sets, and we show how new finite type fractals can be constructed. For finite type self-affine tiles in the plane we give an algorithm which decides whether the tile is homeomorphic to a disk.

1. Introduction. In fractal geometry, the theory of measure and dimension is well-developed. It is possible to determine the Hausdorff dimension, and sometimes even exact Hausdorff measures, for rather complicated fractals sets. Much less is known on the topology of fractals. Even for simple self-affine tiles in the plane, it is not easy to decide whether they are homeomorphic to the unit disk (see Section 6), and in dimension > 2 even connectedness is a problem [1, 22]. For random fractals, it remains a central question to develop a perfect theory of percolation which describes the evolution of connected components in a parametrized fractal construction. In dimension 3 and higher, even the structure of deterministic fractals has not been studied. There is a demand to develop analysis on fractal spaces, in order to deal with physical phenomena like heat and electricity flow in disordered media, vibrations of fractal materials and turbulence in fluids. Without a better understanding of the topology of fractals, this seems very difficult.

In the present paper we study *a class of self-affine fractals for which the topology can*

2000 *Mathematics Subject Classification*: Primary 28A80; Secondary 51M20, 37F20, 68Q70.
M. Mesing was supported by a grant of the Ministry of Culture of Mecklenburg-Vorpommern.
The paper is in final form and no version of it will be published elsewhere.

be described with finite amount of information. The most common examples of fractals, like von Koch's curve, Sierpiński's gasket and Menger's sponge, belong to this class. The concept of finite type has been studied previously in the context of patterns and tilings, see [23]. For fractals, a similar concept has been suggested by Ngai and Wang [30], and several modifications were worked out by Lau and co-workers [13, 24] with the intention to determine Hausdorff dimension for large classes of fractals. Our goal is somewhat different.

We give a very clear definition. *A type is a standardized relative position of two intersecting pieces of the fractal.* These types can be expressed by so-called neighbor maps, which can be explicitly determined by a recursive algorithm. If there are only finitely many neighbor maps, the algorithm stops after finite time, and we have a finite type fractal.

The algebraic structure of neighbor maps will not only determine the Hausdorff dimension of the boundary of the fractal, which has been noted by many authors [33, 24, 14, 20], using more complicated concepts like contact matrices. It will also describe the topological structure of the fractal, in terms of an equivalence relation on the shift space of addresses introduced in [18, 8, 11, 21].

Our definition of finite type leads to a construction of corresponding examples. We give some new examples of fractals with rather simple structure. We also show how the topology of two- and three-dimensional self-affine tiles can be determined by algebraic operations with the data.

2. The neighbor concept. We consider contracting affine maps f_1, \dots, f_m on \mathbb{R}^d , that is, $f_i(x) = A_i(x + v_i)$ where A_i is a $d \times d$ matrix with eigenvalues of modulus < 1 , and $v_i \in \mathbb{R}^d$ is a translation vector. The *self-affine set* corresponding to f_1, \dots, f_m is the unique compact set $F \neq \emptyset$ which satisfies the set equation

$$F = f_1(F) \cup \dots \cup f_m(F) .$$

If the f_i are similarity maps with respect to Euclidean metric, F is called self-similar. F consists of small copies $F_i = f_i(F)$ of itself, each F_i consists of smaller copies $F_{ij} = f_i(f_j(F))$, and so on. For any integer n , we can consider the set S^n of words $\mathbf{i} = i_1 \dots i_n$ from the alphabet $S = \{1, \dots, m\}$. Writing $f_{\mathbf{i}} = f_{i_1} \dots f_{i_n}$ and $F_{\mathbf{i}} = f_{\mathbf{i}}(F)$, we have $F = \bigcup \{F_{\mathbf{i}} \mid \mathbf{i} \in S^n\}$. When n tends to infinity, this induces a continuous map $\pi : S^\infty \rightarrow F$ from the set S^∞ of sequences $\mathbf{s} = s_1 s_2 s_3 \dots$ onto the self-similar set, the so-called address map, cf. [18, 11, 21].

To obtain a reasonable structure in the self-affine set, it is often required that overlaps of the pieces are sufficiently thin, which is expressed by the *open set condition*: there exists a nonempty open set $V \subset \mathbb{R}^d$ with $\bigcup_{i=1}^m f_i(V) \subseteq V$ and $f_i(V) \cap f_j(V) = \emptyset$ for $i \neq j$.

In this paper we give a more detailed study of the relation between small neighboring pieces $F_{\mathbf{i}}$ and $F_{\mathbf{j}}$ of F . When we use the term "neighboring pieces", we shall always assume that $F_{\mathbf{i}} \cap F_{\mathbf{j}} \neq \emptyset$, and we shall call such a pair $F_{\mathbf{i}}, F_{\mathbf{j}}$ "a type". Since we are interested in the relation and not in the size of the pieces, each type is represented in a standard form, taking the fractal F in place of $F_{\mathbf{i}}$ and a virtual neighbor $h(F)$ instead of $F_{\mathbf{j}}$.

Figure 1 shows a very simple self-affine set with three pieces - a triangle with angles

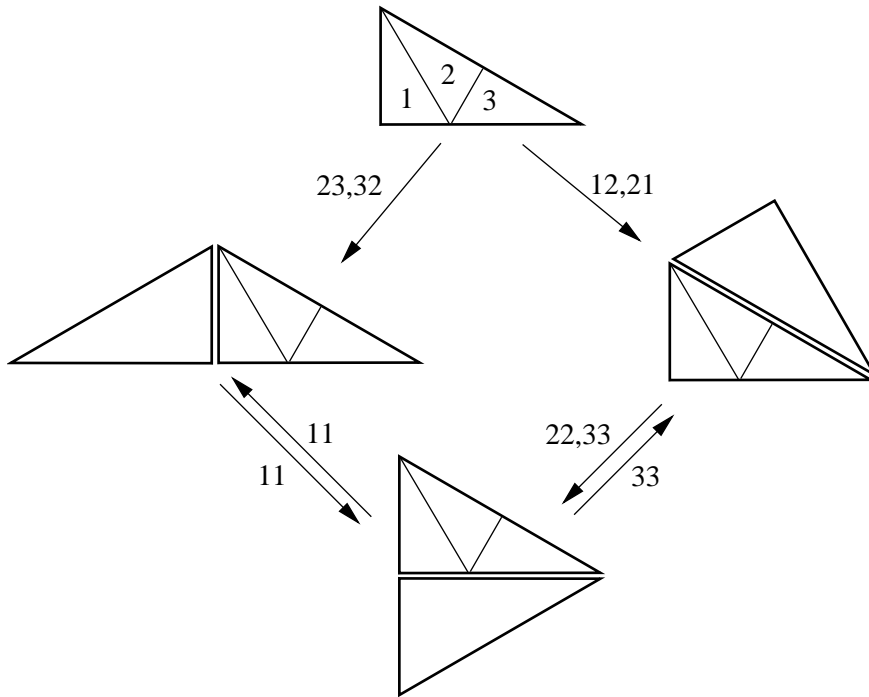


Figure 1: Types of a self-affine triangle

of 30, 60 and 90 degrees. Two small triangles in F can intersect along a line segment, or within a point. Let us neglect the latter case and only consider the "edge neighbors". There are three types of such neighboring triangles. When we put the first triangle into the position of the set F (indicated by the subdivision), then the three neighboring positions are obtained by reflection of F along its three sides.

As Figure 1 shows, two of the types are found among the first-level pieces, that is, F_1, F_2 and F_2, F_3 . The third neighbor pair appears at second level. We can take F_{12}, F_{22} as well as F_{13}, F_{33} or F_{21}, F_{31} . It is clear that we can find all neighbor positions by searching small pieces on both sides of $F_1 \cap F_2$ and $F_2 \cap F_3$, since from such pairs of intersecting triangles, all other pairs are obtained by applying the maps f_i . On the first level, we had found two types, and by studying their subpieces, the third type was discovered. Now considering the subpieces 1, 1 and 3, 3 of the third type, we are led back to the two other types. This shows that we really have only three types of neighboring triangles, no matter how far we go into tiny subpieces. (Inclusion of "point neighbors" like F_1, F_3 , means 13 other types, cf. [17], Figure 2.7.1, tiling [4, 6, 12].) Thus we have a simple recursive method to determine all types of neighboring pieces - at least in the case when only few types exist.

3. The neighbor graph and its algebraic construction. Our intuitive discussion will now be replaced by an algebraic framework which determines the types from the

data of the given maps. Given f_1, \dots, f_m , a *neighbor map* has the form $h = f_i^{-1}f_j$ where $F_i \cap F_j \neq \emptyset$. We imagine that h maps the large fractal F onto a potential neighbor set $h(F)$ which has the same position with respect to F as F_j has with respect to F_i . In fact, f_i maps F to F_i and $h(F)$ to F_j . Our standardization which assumes the first neighbor always to be F is necessary in order to compare different neighbor maps. Working with equivalence classes of neighboring positions, as in [30, 13], is an alternative, but seems to be more complicated.

We are interested in maps between neighbors of (almost) equal size. So in our paper where the f_i have the same linear part, $A_i = A$, or the same contraction factor in the case of similarities, we shall require that the words \mathbf{i} and \mathbf{j} have the same length. It will then turn out that the neighbor maps are isometries. In the case of Figure 1, they were reflections. For the case $A_i = A$, Proposition 1 below says that they are translations.

Neighbor maps can be generated recursively. We start with $f_{i_1}^{-1}f_{j_1}$ where $i_1 \neq j_1$. When a neighbor map $h = f_i^{-1}f_j$ is constructed, the neighbor maps for the pieces F_{i_n} and F_{j_n} of F_i and F_j , respectively, is given as

$$g = f_{i_n}^{-1}f_i^{-1}f_jf_{j_n} = f_{i_n}^{-1}hf_{j_n}.$$

Thus we obtain all neighbor maps by applying repeatedly the interior automorphisms $\Phi_{ij}(h) = f_i^{-1}hf_j$ of the isometry group of \mathbb{R}^d , starting with id . The identity map describes the trivial type of two equal pieces, like F_i, F_i . As drawn in Figure 1, it will always be the starting point of our procedure.

How can we verify the assumption $F_i \cap F_j \neq \emptyset$, in other words, $F \cap h(F) \neq \emptyset$? We may assume that $0 \in F$, by taking 0 as the fixed point of f_1 . Then $F \cap h(F) \neq \emptyset$ is only possible if $\|h(0)\| \leq 2 \operatorname{diam} F$. From the fixed points of the f_i , it is easy to find upper bounds b for the diameter of F so we have the necessary condition $\|h(0)\| \leq 2b$. This condition is also sufficient in the following sense: if $F \cap h(F) = \emptyset$ then the minimal distance between points of F and $h(F)$ is $\varepsilon > 0$. If all f_i have contraction factor $\leq r$, it is easy to check that for any $g = f_i^{-1}hf_j$, the distance between F and $g(F)$ is $\geq \varepsilon/r$, and after several steps this will be $\geq 2b$. See [3, 25, 9] for details.

Thus the selection of neighbor maps is as follows. Consider only those h with $\|h(0)\| \leq 2b$. Let these maps form the vertex set of a graph. The edges of the graph lead from each h to each $g = f_i^{-1}hf_j$, with $i, j \in S$ and $\|g(0)\| \leq 2b$, and are labelled with the corresponding pair of symbols i, j . Finally, we reduce the graph by considering only those vertices h from which an infinite or eventually cyclic path in the graph will start. id denotes the root vertex of this graph G , and the loops from id to id with labels ii will not be drawn, for convention.

The graph G will be called the *neighbor graph* of the family f_1, \dots, f_m , or of the fractal F . We say that F is of *finite type* if the graph G is finite. In this case, from each vertex there starts a path which ends in a directed cycle.

The construction of the neighbor graph and the check of the finite type property can be done by computer, given the data of the f_i . On the other hand, we can determine the f_i in such a way that the neighbor graph G has certain prescribed cycles and is of finite type. Both methods will be demonstrated for the case of small neighbor graphs. They simplify in the case that all f_i have the same linear part:

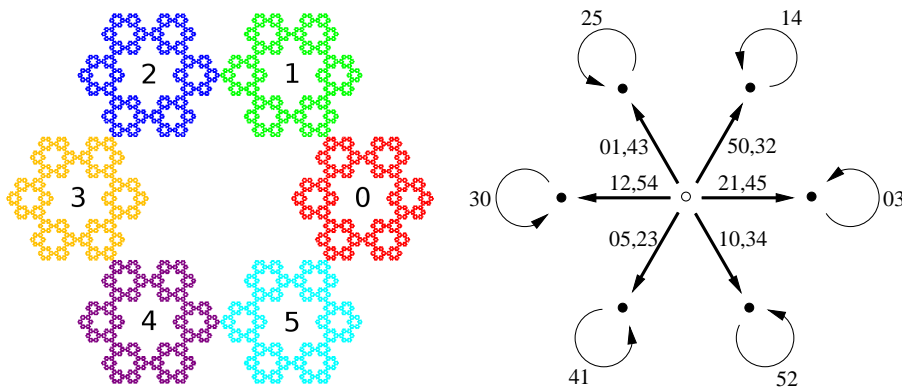


Figure 2: The hexagasket and its neighbor graph

PROPOSITION 1. *If $f_j(x) = A(x + v_j)$ for $j = 1, \dots, m$, all neighbor maps are translations.*

Proof. In this case $f_i^{-1}f_j(x) = x + (v_j - v_i)$, and for $h(x) = x + v$ we get $f_i^{-1}hf_j(x) = x + A^{-1}v + (v_j - v_i)$. \square

As a first example, we consider the hexagasket which was used by Lindstrøm [26] to define a fractal Brownian motion and studied by Strichartz [32] in connection with isoperimetric estimates. The mappings are $f_j(z) = \frac{1}{3}(z + 2b^j)$ for $j = 0, 1, \dots, 5$ where $b = \exp \frac{i\pi}{3}$. In other words, we have homotheties with factor $\frac{1}{3}$ and with fixed points in the sixth roots of unity. As can be seen immediately from Figure 2, the neighbor maps are translations by twice the sixth roots of unity. So we can arrange the vertices of the neighbor graph in such a way that they coincide with the corresponding translation vectors. For example, the identity corresponds to the point zero.

In contrast to Figure 1, here each pair of neighbors corresponds to two neighbor maps: 12 is different from 21. Moreover, each neighbor map is realized by two pairs of first-level pieces (indicated by fat edges with two labels like 50 and 32, instead of drawing double edges). When we go to smaller levels, only one pair of intersecting pieces is available, and the standardized translation is the same as before. Note that when we add a seventh piece in the middle of the gasket, the neighbor graph does not change, only a few more labels have to be added.

4. The identification of addresses. The existence of a continuous projection $\pi : S^\infty \rightarrow F$ from the space of symbol sequences $\mathbf{s} = s_1s_2s_3\dots$ onto the fractal F implies that F is a quotient space of S^∞ . Let us write $s \sim t$ if $\pi(s) = \pi(t)$.

PROPOSITION 2. *If the open set condition holds, all equivalence classes of addresses are finite.*

Proof. Schief [31] has shown that in case of the open set condition, there exists a constant K such that no more than K pieces F_i of (approximately) the same size can have a common point. (Actually, his condition was even stronger.) If more than K sequences in S^∞ are mapped to the same point x , we find an integer n_0 such that all the prefixes of

length n of the sequences are different for $n > n_0$. Corresponding pieces of approximately the same size can now be constructed. They all contain x , which contradicts the open set condition. \square

PROPOSITION 3. *The pairs of equivalent addresses coincide with the label sequences of infinite edge paths in the neighbor graph.*

Proof. The neighbor graph contains an edge from the root id labelled i_1j_1 to some vertex h_1 if and only if $F_{i_1} \cap F_{j_1} \neq \emptyset$. There is an edge from such an h_1 to some h_2 labelled i_2j_2 iff $F_{i_1i_2} \cap F_{j_1j_2} \neq \emptyset$, and so on. Thus there is a path from the root with labels i_1j_1, \dots, i_nj_n if and only if $F_{i_1\dots i_n} \cap F_{j_1\dots j_n} \neq \emptyset$. In the limit, an infinite path s_1t_1, s_2t_2, \dots in the graph corresponds to two addresses $s_1s_2\dots$ and $t_1t_2\dots$ which describe the same point: $\pi(\mathbf{s}) = \pi(\mathbf{t})$. \square

If the neighbor graph is finite, the set of labels i_1j_1, \dots, i_nj_n of finite paths forms a *regular language* on the alphabet $S^2 = \{ij \mid i, j \in S\}$. This concept comes from theoretical computer science where a rooted directed edge-labelled finite graph is also called a *finite automaton*, and is one method to define a regular language. Since we are interested in addresses, we shall use the term "language" for the set of words as well as for the set of sequences which are obtained as limits of these words, that is, from label sequences of infinite paths in the graph. We proved

THEOREM 4. *For a finite type fractal, the equivalence relation \sim of addresses is defined by the regular language on S^2 given by the neighbor graph.* \square

Of course, the infinite paths s_1t_1, s_2t_2, \dots in a finite neighbor graph must contain repeated cycles. So the structure of F depends very much on the relationship of cycles in the neighbor graph. This will be shown in the next section, but one important case has to be mentioned here. Neighbor maps were introduced in [4] to give the following algebraic equivalent of the open set condition: *the identity map cannot be approximated by neighbor maps $f_i^{-1}f_j$* . In particular, a finite type fractal fulfils the open set condition if there is *no edge in G which leads back to id* .

Let us now consider only the first symbol i of the label ij on each edge. Then a path starting in id and labelled $i_1i_2\dots$ gives the address of a point in an intersection set $F_{i_1} \cap F_{j_1}$. However, instead of intersection sets $F_i \cap F_j = D$ we prefer to consider *boundary sets* $f_i^{-1}(D)$. These are the sets $F \cap h(F)$ where the whole fractal F touches a possible neighbor $h(F)$. Moran [29] used the name "dynamical boundary". In the case of a tile F , these boundary sets do indeed cover the topological boundary of F . For a disk-like tile in the plane, all boundary sets are arcs or points. See Section 6.

Except for the root, each vertex h of the neighbor graph corresponds to a boundary set $F \cap h(F)$, and the first labels $i_1i_2\dots$ of the infinite paths *starting in h* give the addresses of the points of this boundary set. This shows

THEOREM 5. *For a finite type fractal with open set condition, the addresses of the boundary set corresponding to h form the regular language L_h defined by the first labels on the graph $G \setminus \{id\}$ with initial vertex h .* \square

EXAMPLE 1. In Figure 1, the boundary sets of the triangle F are the three sides. Let B, C, D denote the shortest, medium, and longest side, respectively. Figure 1 shows that

$$B = f_1(C), \quad C = f_1(B) \cup f_3(D), \quad \text{and} \quad D = f_2(C) \cup f_3(C)$$

from which it follows that

$$C = f_1 f_1(C) \cup f_3 f_2(C) \cup f_3 f_3(C) .$$

f_i has contraction factor $\frac{1}{\sqrt{3}}$, so $f_i f_j$ has factor $\frac{1}{3}$ and C has similarity dimension 1.

Many authors have noted that the boundary sets of self-affine fractals form a graph directed construction [28], and so the Hausdorff dimension of the boundary sets can be calculated (see [33, 24, 14, 20] and the references there). In our framework, however, the graph G of the boundary sets is obtained in a very natural and simple way.

Note that the open set condition for the graph-directed system of boundary sets can be derived from the open set condition for F since the subdivision of boundaries is induced by the partition of F into the F_i . This fact was used by the authors who determined the Hausdorff dimension of boundary sets.

Actually, the definition of finite type by Ngai and Wang [30] depends on the existence of an open set and includes all examples with open set condition (see also [24, 13]). There is an example of Kenyon [19] who took the self-similar 3×3 -division of the square and shifted the third column by a small irrational vertical translation. This example fulfils the open set condition and so has finite type in the sense of [30] but not in our sense.

Our concept is derived from the notion of finite type in patterns and tilings [23] which states that a tile should have only finitely many neighborhoods of surrounding tiles. In fact, if there are only n possible neighbors then there can be at most 2^n possible systems of surrounding neighborhoods. Counting neighbors and counting neighborhoods are *two different concepts of measuring complexity* of a finite type fractal. It can happen that there are less neighborhoods than neighbor maps. For the (essentially unique) tiling generated by Example 1, there is only one possible neighborhood if only fully surrounded tiles are taken into account, while Figure 1 shows three neighbors, and there are 13 neighbors which touch F in a point [17, Figure 2.7.1].

5. Different classes of finite type fractals. Now we study the topological structure of the boundary sets of finite type fractals. *We shall distinguish three classes: finitely ramified, infinitely ramified and overlapping fractals.* Some of the following statements were already given in [3] where neighbor graphs were introduced implicitly.

According to the construction of G , from each vertex h there starts at least one infinite path which in a finite graph must contain repeated cycles. A *terminal cycle* in G is a directed cycle without any diagonal edge or double edge or any edge leading out of the cycle. *Each vertex g on a terminal cycle represents a one-point boundary set, with a single periodic address given by the first labels of the cycle.* Examples are the loops in the neighbor graphs of Figure 2 and the loop at k in Figure 3, and the terminal two-point cycles (f, g) in Figure 7 and $(17, 18)$ in Figure 8.

A vertex h of G is called *terminal vertex* if only terminal cycles can be reached from h . If n paths to terminal cycles start in the terminal vertex h , then this vertex represents

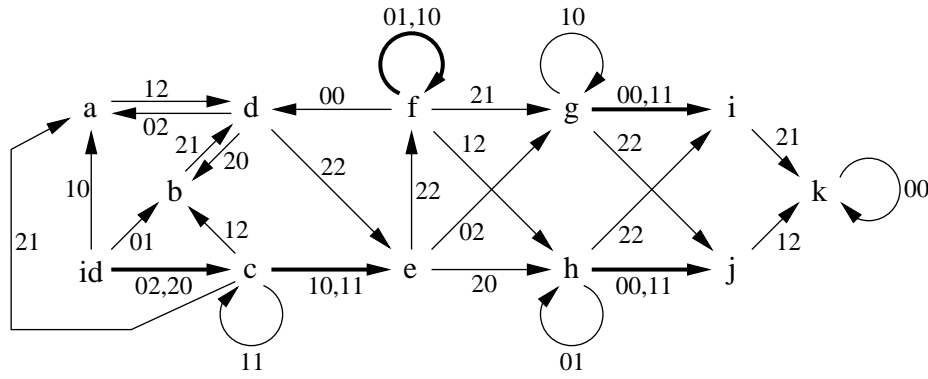


Figure 3: A neighbor graph with different boundary types

a boundary set of n points, all with preperiodic addresses.

Following terminology of Thurston on Julia sets, Kigami [21] calls a self-affine set F *post-critically finite* if all intersection sets $F_i \cap F_j$ are finite, and the points in the intersection have eventually periodic addresses.

PROPOSITION 6. *A finite type fractal is post-critically finite iff all cycles in the neighbor graph are terminal cycles.*

This proposition covers the hexagasket (Figure 2) as well as the Sierpiński gasket and many examples in the literature [21, 32, 6]. The "if"-part was proved above, the "only if"-part will follow from the argument below. Moreover, each post-critically finite fractal defines a finite neighbor graph on a topological level. However, it is not clear whether every realization of this graph by a self-affine set must be of finite type.

Let us call a directed cycle C in G a *multiple cycle* if it contains a double edge (drawn as an edge with at least two labels), or there exist a path between two vertices of C , or a further cycle from one vertex of C to itself, which is disjoint from the edges of C . Examples are the cycles (a, d) , (b, d) , and (d, e, f) in Figure 3, the outer cycle in Figure 4, and the cycles in Figure 5. Multiple cycles always represent uncountably many addresses. In fact, starting with a vertex of C where the second cycle begins, each sequence of words u and v defines one address, where u denotes the labels along C , and v denotes the labels along the cycle with the other edge or diagonal path or cycle excursion.

Each vertex in G from which a multiple cycle can be reached is called a *multiple vertex*. If a vertex is neither a terminal nor a multiple vertex, it is called *intermediate*. Intermediate vertices are those from which we can only reach terminal or intermediate cycles. Here intermediate cycle means a cycle from which a path leads away, but not to a multiple cycle or back to the original cycle. Two such intermediate cycles are the loops at g and h in Figure 3, while the loop at f is a multiple cycle. Thus the vertices i, j , and k in Figure 3 are terminal, the vertices g and h are intermediate, and the other five vertices (without the root) are multiple vertices. See Example 4 below.

THEOREM 7. *In the neighbor graph of a finite type fractal F with open set condition,*

- *terminal vertices represent finite boundary sets,*
- *intermediate vertices represent countably infinite boundary sets, and*
- *multiple vertices represent uncountable boundary sets.*

Proof. We had already seen that terminal vertices describe finite boundary sets, and multiple vertices represent an uncountable number of addresses and thus by Proposition 2 an uncountable boundary set. Now take an intermediate vertex h and a path from h which passes the intermediate cycles C_1, \dots, C_{n-1} and leads to the final cycle C_n . There are only finitely many choices of the C_i since there are only finitely many cycles in G , and the order of intermediate cycles is fixed, by definition. The possible addresses of the boundary set of h now have the form $u_1 c_1^{k_1} u_2 c_2^{k_2} \dots u_r c_r^{k_r}$ where $1 \leq r \leq n$, u_i describes the labels on the path from C_{i-1} to C_i , and c_i describes the labels along the cycle C_i . These are countably many addresses, so by Proposition 2 the boundary set associated with h is countable. \square

In the sequel we shall study the structure of infinite boundary sets more precisely: when do we have Cantor sets, intervals, or surfaces in higher-dimensional fractals?

EXAMPLE 2. *In Figure 4, we have only one multiple cycle, and each double edge marks the division of the boundary set into two disjoint parts. Thus all boundary sets are Cantor sets, in fact self-similar linear Cantor sets with two pieces.*

Let us point out how the mappings for this example were found. We assumed $f_j(z) = \lambda(z + \mathbf{i}^j)$ for $j = 0, 1, 2, 3$. The complex factor λ was constructed from the neighbor graph. We have $f_k^{-1} f_j(z) = \mathbf{i}^j - \mathbf{i}^k$, and for a translation $h(z) = z + v$ we get

$$f_k^{-1} h f_j(z) = z + \frac{v}{\lambda} + \mathbf{i}^j - \mathbf{i}^k .$$

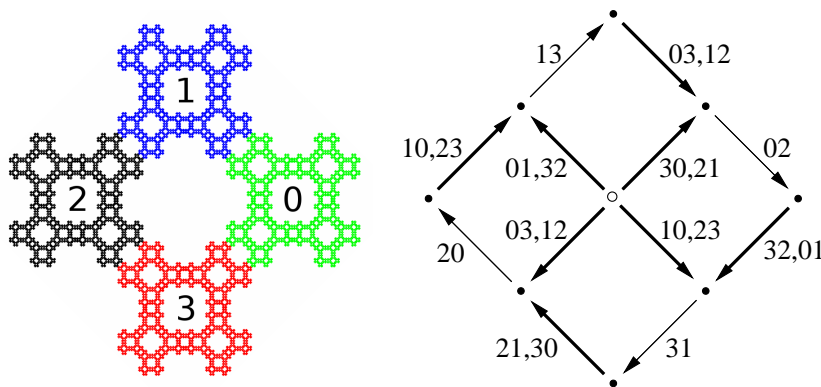


Figure 4: Infinitely ramified square and its neighbor graph

Now going from the upper left vertex in the neighbor graph (which represents the translation vector $\mathbf{i} - 1$) to the right, first up and then down, we obtain the equation

$$\left(\frac{\mathbf{i}-1}{\lambda} + \mathbf{i}^3 - \mathbf{i}\right)/\lambda + \mathbf{i}^2 - \mathbf{i} = \mathbf{i} + 1$$

which leads to the quadratic equation $\lambda^2 + \frac{1+\mathbf{i}}{2}\lambda = \frac{\mathbf{i}}{2}$. The solution is

$$\lambda = \frac{1+\mathbf{i}}{2}\tau \quad \text{with} \quad \tau = \frac{\sqrt{5}-1}{2} \approx 0.618.$$

The other solution has modulus > 1 . So the neighbor graph, together with the assumption of rotational symmetry (cf. [6]) uniquely determines the mappings.

It should be noted that not every given neighbor graph leads to a solution, since sometimes $|\lambda|$ is too large, and we obtain more neighbor maps than we assumed. Nevertheless, we found quite a number of new simple fractals by this method, cf. [3].

We conclude this section with an example of a self-similar fractal with overlap. Overlapping constructions have been studied in several papers [12, 24, 30]. Although they do not fulfil the open set condition, they satisfy a so-called weak separation condition, and their Hausdorff dimension can be determined. The most interesting example seems to be the golden gasket which is generated by three homotheties with factor $\tau = \frac{\sqrt{5}-1}{2} \approx 0.618$. The Hausdorff dimension of the golden gasket is $d = \frac{\log \beta}{\log \tau} \approx 1.93$ where $\beta \approx 0.395$ fulfils the equation $3\beta - 3\beta^3 = 1$ [12]. This can be seen from the method in our next example.

EXAMPLE 3. In the example of Figure 5, we have exactly overlapping pieces $F_{211} = F_{133}$ since the path with labels 21, 13, 13 leads from id back to id . In fact, beside id , the type of two identical pieces, we have only two other classes of overlapping types: neighbors which overlap in pieces of the next level, and neighbors which overlap in pieces which are two levels down. Thus the structure seems simpler than the golden gasket where neighbors may also intersect in a point.

When we assume $f_j(z) = \lambda(z + \mathbf{i}^j)$ for $j = 0, 1, 2, 3$ as in Example 2, we can obtain λ

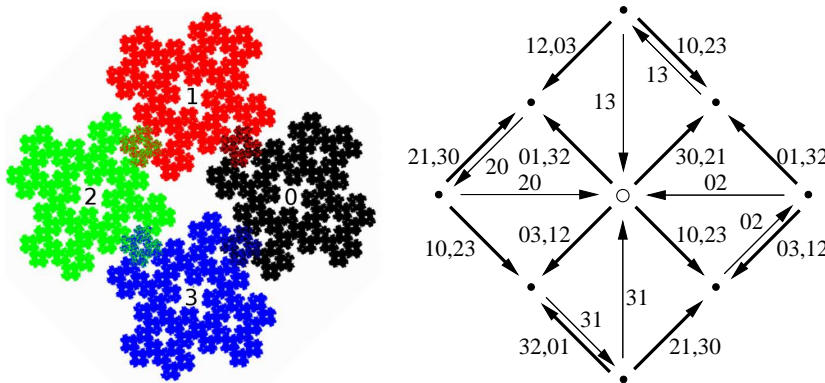


Figure 5: Overlapping square and its neighbor graph

from the equation $f_{211} = f_{133}$, or from the cycle in the neighbor graph just mentioned:

$$\left(\frac{\mathbf{i} - \mathbf{i}^2}{\lambda} + \mathbf{i}^3 - \mathbf{i}\right)/\lambda + \mathbf{i}^3 - \mathbf{i} = 0$$

leads to the quadratic equation $\lambda^2 + \lambda = \frac{1-\mathbf{i}}{2}$. The solution with modulus < 1 is

$$\lambda = -\frac{1}{2} + \sqrt{\frac{3}{4} - \frac{\mathbf{i}}{2}} \approx 0.409 - 0.275\mathbf{i}.$$

To determine the Hausdorff dimension of F , assume there is a normalized d -dimensional Hausdorff measure μ on F . Then $\mu(F) = 1$, and $\mu(F_i) = r^d$, $\mu(F_{ijk}) = r^{3d}$ with $r = |\lambda|$. Putting $\beta = r^d$ we get $4\beta - 4\beta^3 = 1$ since the measure of F is the sum of the measures of the F_i minus the measure of those pieces which have been counted twice. Since $\beta < \frac{1}{2}$, the solution is $\beta \approx 0.2696$ and $d = \frac{\log \beta}{\log r} \approx 1.85$. The method in [12] can be used to confirm this result.

6. Disk-like tiles. We are going into a detailed study of the topology for a special case: self-affine sets with non-empty interior and open set condition, which are called *self-affine tiles*. Extending the self-similar construction to the outside, we can construct *self-affine tilings* of \mathbb{R}^d , that is, we cover the whole space by non-overlapping copies $h_k(F)$ of F so that $\mathbb{R}^d = \bigcup_{k=1}^{\infty} h_k(F)$. Such tilings have been studied intensely because of their aperiodicity, see [17, Chapter 10]. For us, examples of tilings gave a strong motivation to develop the neighbor graph.

Self-affine tilings on \mathbb{R}^d can be generated from an integer matrix B with determinant m such that $g(x) = Bx$ is expanding (i.e. has eigenvalues of modulus > 1), and m vectors v_i in the integer lattice \mathbb{Z}^d such that $g(\mathbb{Z}^d) + \{v_1, \dots, v_m\} = \mathbb{Z}^d$. We then have

$$g(F) = \bigcup_{k=1}^m v_k + F \quad \text{or} \quad F = \bigcup_{k=1}^m f_k(F) \quad \text{with} \quad f_k(x) = B^{-1}(x + v_k).$$

A more general and interesting construction uses an arbitrary crystallographic group Γ acting on \mathbb{R}^d [16]. That is, Γ contains a maximal abelian subgroup Λ which is a normal subgroup of finite index in Γ and is isomorphic to \mathbb{Z}^d . A crystallographic reptile [16] is defined by a crystallographic group Γ acting as a group of isometries on \mathbb{R}^d , by an expanding affine map $g : \mathbb{R}^d \rightarrow \mathbb{R}^d$ with determinant $\pm m$ for which $g\Gamma g^{-1} \subseteq \Gamma$, and, finally, by group elements $\gamma_1, \dots, \gamma_m$. The reptile is the set F which fulfils

$$g(F) = \bigcup_{j=1}^m \gamma_j(F) \quad \text{or} \quad F = \bigcup_{j=1}^m f_j(F) \quad \text{with} \quad f_j = g^{-1}\gamma_j.$$

Since $f_k^{-1} = \gamma_k^{-1}g$, the neighbor maps are elements of Γ , determined recursively from $f_k^{-1}f_j = \gamma_k^{-1}\gamma_j$ and $\Phi_{ij}(\gamma) = f_k^{-1}\gamma f_j = \gamma_k^{-1}\gamma\gamma_j$. So the finite index condition in the definition of Γ implies that F is of finite type.

For a reptile it is required that the identity map is not obtained as a neighbor map $f_k^{-1}f_j$ with $k_1 \neq j_1$. Then by [4] the open set condition is fulfilled, F has non-empty interior, and there is a tiling $\mathbb{R}^d = \bigcup_{\gamma \in \Gamma_0} \gamma(F)$ with $\Gamma_0 \subseteq \Gamma$, cf. [16, Theorem 3.5]. In [16, 27] reptiles are required to fulfil $\Gamma_0 = \Gamma$, so that the tiling is tile-transitive with automorphism group Γ . However, we can deal with the more general case which also

includes the well-known self-similar tilings by chair and sphinx [17, Chapter 10],[16, Remark 3.9].

For geometers working with tilings it goes without saying that a tile in the plane should be homeomorphic to a disk. However, fractal constructions often lead to tiles which are either disconnected or have holes or cutpoints, or still more intricate structure, as for instance the Lévy curve [14, 20]. Thus it is very natural to ask *which self-affine tiles are disk-like*. For lattice tiles in the plane this is not too hard to decide [10, 5]. For crystallographic tiles, however, the question is still unsolved although partial answers have been given [27]. Loridant, Luo, and Thuswaldner use an infinite lattice-type graph which they call neighbor graph. It is related with, but different from our construction.

It should be noted that from computer pictures, like Figure 6 and 8, we can often not decide whether a self-affine tile is disk-like. In particular when the contracting eigenvalues of the mappings f_i are different, which is the case in Figure 6, an intricate fibre structure is obtained which is blurred by iteration algorithms used to draw fractals. Usually the appearance of a tile is too fat, and if the neighbors are added, it becomes too meagre. Even more precise algorithms, as described in [11], do not provide sufficient resolution, so that exact methods are indispensable.

Here we show how the question of disk-likeness can be answered for all plane self-affine tiles. We use formal calculations based on the neighbor graph and regular languages, without referring to Jordan curve arguments. So in principle our methods also apply to higher dimensions! However, the calculations are pretty complicated and are best delegated to a computer. We apply our method to two tiles for which Gelbrich [16] asked whether they are disk-like.

EXAMPLE 4. *Sometimes the neighbor graph shows directly that a tile is not disk-like. The tile in Figure 6 (originally Figure 8a in [16]) corresponds to the neighbor graph of Figure 3. The mappings are $f_i(x) = A(x + v_i), i = 0, 1$ and $f_2(x) = -A(x + v_2)$ with $A = \frac{1}{3} \begin{pmatrix} 2 & -1 \\ -1 & -1 \end{pmatrix}$ and $v_0 = \begin{pmatrix} 0 \\ -\frac{1}{2} \end{pmatrix}$, $v_1 = \begin{pmatrix} 0 \\ \frac{1}{2} \end{pmatrix}$, and $v_2 = \begin{pmatrix} 1 \\ \frac{1}{2} \end{pmatrix}$. The crystallographic group Γ is generated by integer translations and $\gamma(x) = -x$, the expanding*

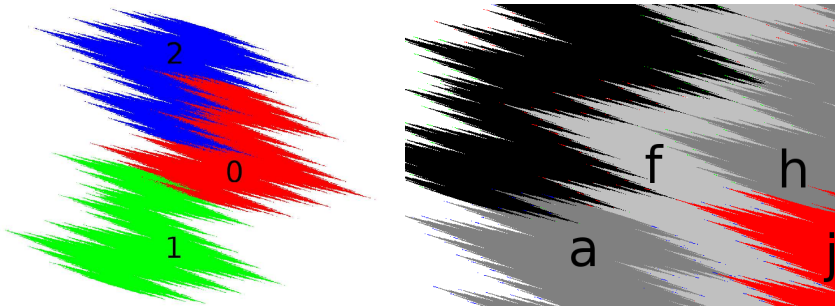


Figure 6: A self-affine tile which is not disk-like. For the neighbor graph see Figure 3.

map is $g(x) = \begin{pmatrix} 1 & -1 \\ -1 & -2 \end{pmatrix} x + \begin{pmatrix} \frac{1}{2} \\ 0 \end{pmatrix}$. The eigenvalues of the expanding matrix are $\frac{1}{2}(-1 \pm \sqrt{10})$, so F is self-affine, not self-similar.

We had seen that there are one-point, countably infinite and uncountable boundary sets. For a disk-like tile, however, it is easy to see that any boundary set is either a point or a topological line segment [16, Lemma 4.1]. So since there is a countably infinite boundary set, the tile is not homeomorphic to a disk. The right-hand part of Figure 6 indicates the position of certain neighbors in the graph of Figure 3. The fractal tile F is drawn in black, and the neighbors denoted a and f intersect the tile in uncountable sets. After our calculation, we can imagine that j is a neighbor which meets the tile in one point, and h meets the black tile in a countable infinite boundary set. j and h divide the interior of the neighbor tile f into many components. The picture alone would not provide enough evidence for these facts.

How can we confirm that a tile is really disk-like? We must check that all boundary sets are either singletons or homeomorphic to an interval. The boundary sets which are singletons are terminal vertices as discussed in Section 4. We could check that they admit only one path to a terminal cycle, but this is only one necessary condition, and here we look for a complete method.

All terminal vertices and also the root vertex id , with all their edges, are now cancelled from the neighbor graph, resulting in the *simplified neighbor graph* G^* , where we take only the first symbols as labels. See Figure 7 for an example.

We now have to show that all vertices in G^* represent intervals. Let us first consider the case that the tiling is tile-transitive, $\Gamma_0 = \Gamma$, as required in [16, 27]. For a boundary set associated with the neighbor map h , we denote with L_h the regular language of all its addresses which by Theorem 5 is given by the first labels of paths starting in the vertex h .

THEOREM 8. *The following conditions for the simplified neighbor graph G^* are necessary and sufficient for the transitive reptile F to be disk-like.*

- (1) *The vertices of G^* can be arranged in cyclic order h_0, \dots, h_{n-1} such that the associated regular languages L_k and L_{k+1} (+ modulo n) meet exactly in one address, or in one equivalence class of \sim , and the L_k are disjoint otherwise. The corresponding points of the boundary sets associated with h_k will be called the endpoints of h_k .*
- (2) *The successor vertices of each vertex h in G^* can be linearly ordered so that the boundary sets of consecutive vertices have a common endpoint, and languages of non-consecutive vertices are disjoint. The two endpoints of the boundary set associated with h must be endpoints of the first and last successor vertex.*

Proof. If the tile F is disk-like, the neighbors which intersect F in an interval surround F , and the union of intervals coincides with the topological boundary of F , which is a Jordan curve. Moreover, the intervals generated by two neighbors can have only one point in common, because otherwise the neighbor tiles must have interior points in common, which is not possible in the tile-transitive case. This implies (1). When we now go to pieces

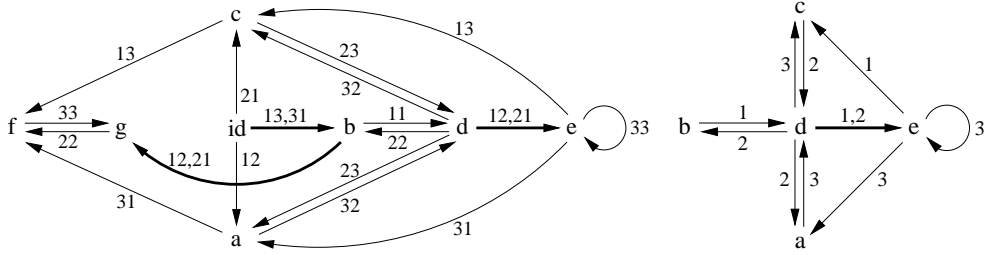


Figure 7: Neighbor graph and simplified neighbor graph of a tile

of F and the neighbors, they also intersect in an interval, and again, these intervals have at most one point in common. These intervals partition the larger intervals, which implies (2).

Now assume that the conditions are fulfilled. We have to prove that the topological boundary ∂F of F is a Jordan curve. Since F is a tile, ∂F is the union of the (dynamical) boundary sets, and is also the union of the infinite boundary sets. Thus when each boundary set H is homeomorphic to an interval, it follows from (1) that ∂F is a Jordan curve.

We use (2) to construct a homeomorphism $\phi : [0, 1] \rightarrow H$. We map 0 and 1 to the two endpoints of H . When h has n successor vertices, in other words, H divides into n pieces, then the endpoints of the pieces which do not agree with $\phi(0)$ and $\phi(1)$ will be defined as $\phi(\frac{1}{n}), \phi(\frac{2}{n}), \dots, \phi(\frac{n-1}{n})$ in such a way that their linear order (or the reverse order, since $\phi(0)$ and $\phi(1)$ were already fixed) agrees with the order of the interval. Now we use (2) to proceed inductively with smaller intervals and subpieces. As a result, we obtain a one-to-one mapping ϕ from a dense subset of $[0, 1]$ onto the set of all endpoints of subpieces of H . This map is continuous since subdivision points of the interval which have distance less N^{-k} (where N denotes the maximum number of successors of a vertex in G^*) must belong to one piece, or two neighboring pieces, of the k -th subdivision of H . So ϕ can be extended to a continuous map from $[0, 1]$ onto H , which is the closure of all endpoints of subpieces of H . This extension is one-to-one since for any number $t \in [0, 1]$ which is not a subdivision point, the pieces of $\phi(t)$ are uniquely determined and so $\phi(t)$ has only one address. A one-to-one map between compact Hausdorff spaces is a homeomorphism. \square

As we see in the following example, the check of (1) and (2) reveals the complete combinatorial structure of the tiling under investigation.

EXAMPLE 5. We consider a self-similar tile introduced by Gelbrich [16, Figure 7b]. The mappings are $f_i(x) = A(x + v_i), i = 1, 2$ and $f_3(x) = -A(x + v_3)$ with $A = \frac{1}{3} \begin{pmatrix} -1 & -1 \\ 2 & -1 \end{pmatrix}$, $v_1 = \begin{pmatrix} \frac{1}{2} \\ 0 \end{pmatrix}$, $v_2 = \begin{pmatrix} \frac{1}{2} \\ 1 \end{pmatrix}$, and $v_3 = \begin{pmatrix} -\frac{1}{2} \\ 0 \end{pmatrix}$. The group is the same as in Example 4.

Figure 7 shows the neighbor graph G and the simplified graph G^* . Let us determine

the languages corresponding to the five boundary sets given by a, b, c, d, e . From vertex d the following cycles go back to d : 23 via a , 21 via b , 32 via c , and $13^*12, 23^*12, 13^*33, 23^*33$ via e . Here 3^* can be empty or any 3^k . The sequences of the language L_d are generated by composing these words:

$$L_d = \{23, 21, 32, 13^*12, 23^*12, 13^*33, 23^*33\}^\infty .$$

The languages of the other vertices are derived from L_d :

$$L_a = 3 \cdot L_d, L_b = 1 \cdot L_d, L_c = 2 \cdot L_d, \text{ and } L_e = \{3^*12, 3^*33\} \cdot L_d .$$

By Theorem 5, these languages consist of the addresses of all points of the corresponding boundary sets. Now we determine their intersections. L_e does not intersect L_d since no word of L_d starts with $12, 31$ or 33 . Similarly, L_b does not intersect L_d since $1w$ with $w \in L_d$ does not give $112, 131$ or 133 . However, $L_c \cap L_d = \{2\bar{3}\}$ and $L_a \cap L_d = \{3\bar{2}\}$.

L_c is disjoint with L_a, L_b, L_e since their words do not begin with 2 . However, the sequences $1\bar{3}\bar{2}$ in L_b and $2\bar{2}\bar{3}$ in L_c are equivalent as can be seen from G . So the boundary sets corresponding to b, c have a single point in common. Moreover, $L_b \cap L_e = \{1\bar{2}\bar{3}\}$, and $L_a \cap L_e = \{3\bar{3}\bar{2}\}$. Thus condition (1) is fulfilled for the cyclic order c, d, a, e, b .

Property (2) need not be checked for a, b , and c , since d is their only successor vertex. e has successors a, e, c with edge labels $3, 3$, and 1 , respectively. $3L_a$ contains the endpoint $3\bar{3}\bar{2}$ of e , and $1L_c$ contains the other endpoint $1\bar{2}\bar{3}$. Starting with different letters, these two languages are disjoint, while $3L_a \cap 3L_e = 3(L_a \cap L_e)$, and $1L_c, 3L_e$ contain the equivalent addresses $12\bar{2}\bar{3}$ and $31\bar{2}\bar{3}$. Finally, d has successors a, b, c , with and two successors e , which can be expressed as

$$L_d = 2L_a \cup 2L_e \cup 2L_b \cup 1L_e \cup 3L_c .$$

The endpoints $\bar{2}\bar{3}$ and $\bar{3}\bar{2}$ of d belong to the first and last part. By (1), among the first three parts only consecutive languages have an address in common, and they are disjoint with the other two parts which have another starting letter. However, the check of \sim shows that $21\bar{3}\bar{2} \in 2L_b$ is equivalent to $13\bar{3}\bar{2} \in 1L_e$, and $11\bar{2}\bar{3} \in 1L_e$ is equivalent to $32\bar{2}\bar{3} \in 3L_c$. So (2) is proved.

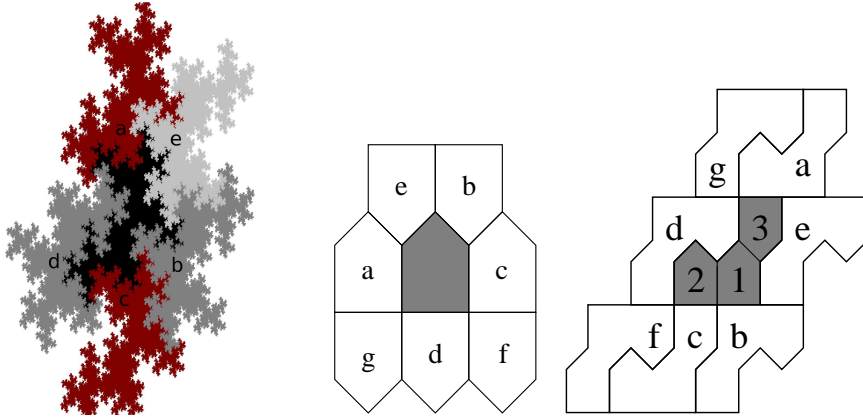


Figure 8: A fractal tile, its combinatorial and self-similarity structure

There exists a topological classification of plane tile-transitive tilings [17, Figure 2.7.1]. Since we have five neighbor types in G^* , and two neighbors which meet F in a point, the structure of our tiling is given by the symbol $[3^3 4^2]$. In Figure 8, the scheme of this tiling and the self-similarity structure of our example is drawn. The correspondence with the above calculations and with the fractal picture is easy to see.

Let us generalize Theorem 8 to the case of arbitrary finite type self-affine plane tilings which need not be transitive or crystallographic. Different neighborhoods are possible, and the number of possible neighbors of F can be much larger than the number of real neighbors of one tile. A new problem is that two boundary intervals can intersect in a whole subinterval when the corresponding neighbors do not actually appear together. This requires a more careful formulation, but the proof is very similar to the proof of Theorem 8 and will not be given here. The condition (1) now says n boundary sets form the topological boundary of F , and so must cover all other boundary sets.

THEOREM 9. *The following conditions for the simplified neighbor graph G^* are necessary and sufficient for a plane self-affine tile F of finite type to be disk-like.*

- (1) *There are vertices of G^* which can be arranged in cyclic order h_0, \dots, h_{n-1} such that the associated regular languages L_k and L_{k+1} (+ modulo n) meet exactly in one address, or in one equivalence class of \sim , and the L_k are disjoint otherwise. For all other vertices g , the language L_g is contained in $\bigcup_{k=0}^{n-1} L_k$.*
- (2) *The successor vertices of each vertex h in G^* can be linearly ordered so that the boundary sets of consecutive vertices have a common endpoint, and languages of non-consecutive vertices are disjoint. The two endpoints of the boundary set associated with h must be endpoints of the first and last successor vertex. For all relations in which some h appears as vertex or successor vertex, the endpoints of h are the same.*

Let us note that even the necessity of the condition is not so obvious. If the tiling is not transitive, it can happen that neighboring tiles meet in two points, enclosing one or two other tiles between them. An example is Voderberg's spiral tile from 1936, cf. [17]. Here we work with neighbors which intersect in an arc, and we need the fact that they cannot intersect in a further point or arc. This follows from the uniqueness argument in Voderberg's paper [34] which, however, is not complete according to contemporary standards of proof. It would be nice to have a more simple argument for this fact.

7. A three-dimensional example. Research on self-similar fractals has been focussing on the plane case: there are very few examples in \mathbb{R}^d with $d \geq 3$. One reason could be that computer visualization is most simple in two dimensions. However, there are also mathematical obstacles. In dimension greater than two, even linear similarity maps will rarely commute. It also turns out that it is not easy to construct finite type examples. For example, it seems that in \mathbb{R}^3 there are no crystallographic self-similar tiles with less than 8 pieces. The reason is that the eigenvalues of a 3×3 integer matrix usually have at least two different moduli.

Moreover, since in \mathbb{R}^3 there is no analogue of the Jordan curve theorem, the topological structure of fractal tiles can be extremely complicated, and so it was not studied so far. We present here a simple example of a three-dimensional self-affine tile with two pieces which seems to be homeomorphic to a ball.

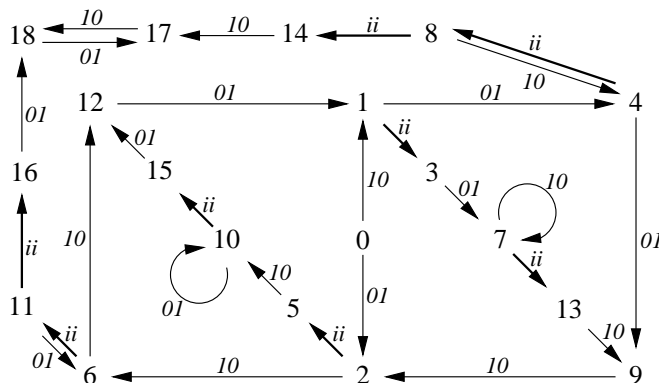


Figure 9: The neighbor graph of a three-dimensional tile

EXAMPLE 6. (A three-dimensional twindragon) In \mathbb{R}^3 we consider the tile F defined by $g(F) = F \cup (F + v_1)$ or $F = f_0(F) \cup f_1(F)$ with $f_0 = g^{-1}$, $f_1(x) = g^{-1}(x + v_1)$, where

$$g(x) = \begin{pmatrix} 0 & 2 & 0 \\ 0 & 0 & 1 \\ -1 & 1 & 1 \end{pmatrix} \quad \text{and} \quad v_1 = \begin{pmatrix} 1 \\ 0 \\ 0 \end{pmatrix}.$$

This is a tile-transitive lattice tile, and it is centrally symmetric (see the argument in [2, Section 5]). Figure 9 shows the neighbor graph which is finite. There are four terminal vertices 14, 16, 17, 18 which represent one-point boundary sets. The other 14 neighbor types describe seven pairs of opposite neighbor sets, interchanged by the central symmetry. They all have the same dimension, since each of these neighbor sets contains copies of each of the other ones.

Our computer pictures of this tile were much worse than the plane Figures 6 and 8. They did not provide any geometrical insight. However, from the neighbor graph it seems very likely that the tile is homeomorphic to a ball, and the 14 faces are homeomorphic to disks. There is a polyhedral space tiling by truncated octahedra, which are centrally symmetric and admit 14 faces, of which 6 are hexagons and 8 are squares [35]. However, these polyhedra have no one-point neighbors.

The neighbor graph is simple enough to derive the graph of all intersections of two faces, which should be edges of our fractal polyhedron. We obtain 40 edges, and when the one-point boundary sets are neglected, they do indeed bound 6 hexagons and 8 squares. Details will be given elsewhere.

References

- [1] S. Akiyama and N. Gjini, *Connectedness of number-theoretic tilings*, Discrete Math. Theoret. Computer Science, to appear
- [2] C. Bandt, *On the Mandelbrot set for pairs of linear maps*, Nonlinearity **15** (2002), 1127-1147.
- [3] C. Bandt, *Self-similar measures*, Ergodic Theory, Analysis, and Efficient Simulation of Dynamical Systems, B. Fiedler (ed.), Springer 2001, 31-46.
- [4] C. Bandt and S. Graf, *Self-similar sets VII. A characterization of self-similar fractals with positive Hausdorff measure*. Proc. Amer. Math. Soc. **114** (1992), 995-1001.
- [5] C. Bandt and G. Gelbrich, *Classification of self-affine lattice tilings*, J. London Math. Soc (2) **50** (1994), 581-593.
- [6] C. Bandt and N.V. Hung, *Fractal n -gons*, Preprint-Reihe Mathematik **11**, Greifswald, 2007.
- [7] C. Bandt, N.V. Hung, and H. Rao, *On the open set condition for self-similar fractals*, Proc. Amer.Soc. **134** (2006), 1369-1374.
- [8] C. Bandt and K. Keller, *Self-similar sets 2. A simple approach to the topological structure of Fractals*, Math. Nachr. **154** (1991), 27-39.
- [9] C. Bandt and H. Rao, *Topology and separation of self-similar fractals in the plane*, Nonlinearity **20** (2007), 1463-1474.
- [10] C. Bandt and Y. Wang, *Disk-like self-affine tiles in \mathbb{R}^2* , Discrete Comput. Geom. **26** (2001), 591-601.
- [11] M.F. Barnsley, *Fractals Everywhere*, 2nd ed., Academic Press 1993.
- [12] D. Broomhead, J. Montaldi, and N. Sidorov, *Golden gaskets: variations on the Sierpiński sieve*, Nonlinearity **17** (2004), 1455-1480.
- [13] Q.-R. Deng, K.-S. Lau, and S.-M. Ngai, *On the finite type condition*, preprint, Hong Kong 2004.
- [14] P. Duvall, J. Keesling, and A. Vince, *The Hausdorff dimension of the boundary of a self-similar tile*, J. London Math. Soc. (2) **61** (2000), 748-760.
- [15] K.J. Falconer, *Fractal Geometry*, Wiley 1990.
- [16] G. Gelbrich, *Crystallographic reptiles*, Geometria Dedicata **51** (1994), 235-256.
- [17] B. Grünbaum and G.C. Shephard, *Tilings and Patterns*, Freeman, San Francisco 1987.

- [18] M. Hata, *On the structure of self-similar sets*, Japan J. Appl. Math. **2** (1985), 281-414.
- [19] R. Kenyon, *Inflationary tilings with a similarity structure*, Comment. Math. Helvetici **69** (1994), 169-198.
- [20] R. Kenyon, J. Li, R.S. Strichartz, and Y. Wang. *Geometry of self-affine tiles II*, Indiana Univ. Math. J. **48** (1999), 25-42.
- [21] J. Kigami, *Analysis on fractals*, Cambridge University Press, 2001.
- [22] I. Kirat, K.-S. Lau, and H. Rao, *Expanding polynomials and connectedness of self-affine tiles*, Discrete Comput. Geom. **31** (2004), 275-286.
- [23] J. C. Lagarias, *Geometric Models for Quasicrystals I. Delone Sets of Finite Type*, Disc. Comp. Geom. **2** (1999), 161-191
- [24] K.-S. Lau and S.-M. Ngai, *A generalized finite type condition for iterated function systems*, Advances Math. **208** (2007), 647-671.
- [25] K.-S. Lau, S.-M. Ngai, and H. Rao, *Iterated function systems with overlaps and self-similar measures*, J. London Math. Soc. (2) **63** (2001), no. 1, 99-116
- [26] T. Lindström, *Brownian motion on nested fractals*, Mem. Am. Math. Soc. **83** (1990), 1-124.
- [27] B. Loridant, J. Luo, and J.M. Thuswaldner, *A new criterion for disk-like crystallographic reptiles*, Topology Proceedings, to appear
- [28] R.D. Mauldin and S.C. Williams, *Hausdorff dimension in graph directed constructions*, Trans. Amer. Math. Soc. **309** (1988), 811-829.
- [29] M. Moran, *Dynamical boundary of a self-similar set*, Fund. Math. **160** (1999), 1-14.
- [30] S.-M. Ngai and Y. Wang, *Hausdorff dimension of self-similar sets with overlaps*, J. London Math. Soc. **63** (2001), 655-672
- [31] A. Schief, *Separation properties of self-similar sets*, Proc. Amer. Soc. **112** (1994), 111-115
- [32] R.S. Strichartz, *Isoperimetric estimates on Sierpiński gasket type fractals*, Trans. Amer. Math. Soc. **351** (1999), 1705-1752.
- [33] J.J.P. Veerman, *Hausdorff dimension of boundaries of self-affine tiles in \mathbb{R}^N* , Bol. Soc. Math. Mexicana (3) **4** (1998), 159-182.
- [34] H. Voderberg, *Zur Zerlegung der Umgebung eines ebenen Bereichs in kongruente*, Jahresber. DMV **46** (1936), 229-231.
- [35] http://en.wikipedia.org/wiki/Bitruncated_cubic_honeycomb